Gem Trade **LAB NOTES**

Editors

Thomas M. Moses, Ilene Reinitz, Shane F. McClure, and Mary L. Johnson
GIA Gem Trade Laboratory

Contributing Editors

G. Robert Crowningshield
GIA Gem Trade Laboratory, East Coast

Karin N. Hurwit, John I. Koivula, and Cheryl Y. Wentzell
GIA Gem Trade Laboratory, West Coast

An Interesting CHAROITE Cabochon

A cabochon of charoite with an interesting inclusion was recently sent to the West Coast lab by gemologist Leon M. Agee of Agee Lapidary in Deer Park, Washington. Mr. Agee told us that the cabochon was cut from a slab discovered in a bin of cutting scraps at the 2001 Tucson gem show. The finished stone weighed 292.14 ct and measured 85.78 × 56.57 × 6.70 mm (figure 1).

While charoite is relatively well known as an ornamental gem material, it was the X-shaped pattern and length (79 mm) of the orangy brown inclusion that made this cabochon interesting. Other inclusions visible with a gemological microscope were transparent and near-colorless, or greenish black. Since all of these inclusions had been exposed on the surface and were nicely polished during lapidary preparation, they presented ideal targets for GIA's laser Raman microspectrometer.

Figure 1. This 292.14 ct charoite cabochon is host to a large X-shaped spray of tinaksite.

The Raman spectrum of the large orangy brown inclusion matched that of the rare mineral tinaksite. We determined that the greenish black inclusions were aegirine, whereas the transparent to translucent near-colorless inclusions proved to be feldspar or quartz, depending on where the testing was done on the polished surface. Although we have examined many objects fashioned from charoite since it was first described as a new mineral in 1976—and encountered aegerine, feldspar, quartz, and tinaksite as inclusions—none of those inclusions had approached this tinaksite in size and unusual shape.

JIK and Maha Tannous

High-Iron Cat's-Eye CHRYSOBERYL

Gem-quality chrysoberyl typically shows consistent optical and physical properties. Although variances in its refractive indices have been reported in the literature—with values sometimes so high that the material could be confused with corundum—such chrysoberyls actually are quite rare. Most gemologists have never seen one.

The West Coast lab recently examined a green chatoyant cabochon that was represented as chrysoberyl from Orissa, India. It was sent to us by K & K International of Falls Church, Virginia. The saturated, slightly yellowish green color of the

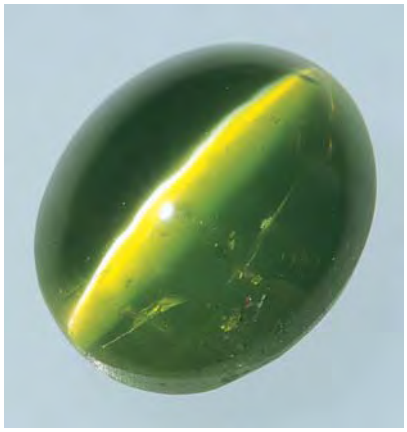

Figure 2. This 4.58 ct cat's-eye chrysoberyl cabochon had extremely high R.I. and S.G. values.

4.58 ct cabochon was very unusual for chrysoberyl, but the eye was strong and typical in appearance of the chatoyancy seen in this species (figure 2). However, when we put the stone on a refractometer, the spot reading was 1.78, much too high for chrysoberyl (usually 1.746–1.755). The specific gravity of the stone, measured hydrostatically, was also high, at 3.81. There was no fluorescence to long- or short-wave ultraviolet radiation, which would be typical for this color of chrysoberyl. The only feature seen with the desk-model spectroscope was a cutoff at about 480 nm.

These properties were somewhat perplexing, so we obtained permission from our client to polish a small flat facet on the back of the stone in order to get a more precise R.I. reading. Accurate refractive indices of 1.780 and 1.793 (birefringence 0.13) were then obtained on the flat polished surface. We were unable to find any reference to a mineral that fit both the physical appearance and the measured properties of the stone in question.

Moving to more sophisticated tests on the cabochon, we obtained a Raman spectrum that matched chrysoberyl exactly. Energy-dispersive X-ray fluorescence (EDXRF) qualitative chemical analysis showed strong peaks for aluminum and iron with minor peaks for titanium, gallium, and tin. Beryllium is too light an element to be detected by EDXRF, so aluminum would be the only major element we would expect to find using this method. Therefore, the presence of a much higher iron content than expected confused the issue further.

However, X-ray powder diffraction also confirmed the mineral to be chrysoberyl. Because this cat's-eye chrysoberyl was the most unusual one we had ever seen, we obtained further permission from the owner to submit it to quantitative chemical analyses by electron microprobe.

The microprobe analyses were carried out by Drs. William "Skip" Simmons and Alexander Falster at the University of New Orleans in Louisiana. In addition to the expected major aluminum content, analyses of 11 different spots on the stone revealed 8.92–10.27 wt.% Fe_2O_3 (as total Fe). Traces of titanium were also detected (up to 0.18 wt.% TiO_2), but all other elements analyzed were at or below the detection limit. The large amount of iron (as compared to 0.5–2 wt.% Fe_2O_3 typically recorded) was clearly the cause of the extremely high R.I.'s and S.G.

Although we were not able to find any reference to a chrysoberyl with comparable refractive indices, birefringence, or S.G., we did note one reference to a cat's-eye chrysoberyl with very similar chemistry in a report by M. Hayashi ("Iron-rich chrysoberyl cat's-eye," *Journal of the Gemmological Society of Japan*, Vol. 19, No. 1–4, 1994, pp. 31–32). That stone had approximately 9.90 wt.% Fe_2O_3 (as determined by EDXRF) with an R.I. of 1.77 and an S.G. of 3.75. Although its iron content was similar to that of the chrysoberyl we examined, the R.I. and S.G. values of that stone were somewhat lower.

Coincidentally, while the anomalous cat's-eye was in the laboratory, we also examined two transparent faceted greenish yellow 0.80 and 1.05 ct chrysoberyls from Joeb Enterprises in Solana Beach, California, that fit the data most often quoted in the literature for high-property chrysoberyl (see, e.g., R. Webster, *Gems*, 5th ed., Butterworth-Heinemann, Oxford, UK, 1994, p. 134; figure 3). Reported to be from Malawi, both of these stones had R.I.'s that nearly matched those of corundum: 1.759–1.769. Although we did not obtain microprobe data on these stones, EDXRF analysis indicated that they also had an iron content that was relatively high for chrysoberyl, although not as high as in the cat's-eye. *SFM*

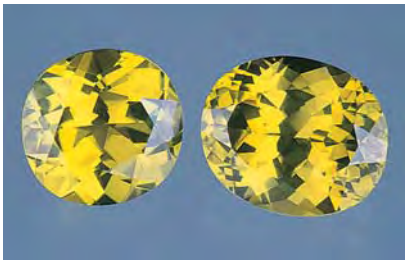

Figure 3. These 0.80 and 1.05 ct greenish yellow chrysoberyls also displayed unusually high properties, but they were still significantly lower than the cat's-eye in figure 2.

DIAMOND, with Unusually Large Laser Drill Holes

The East Coast lab recently received for grading a 3.30 ct near-colorless round brilliant cut diamond. Using a standard gemological microscope and overhead reflected light, we observed three unusual cavities—two on the pavilion and one on the crown. Both were irregular in shape, with the outline of one resembling a flower (figure

Editor's note: The initials at the end of each item identify the editor(s) or contributing editor(s) who provided that item. Full names are given for other GIA Gem Trade Laboratory contributors.

Gems & Gemology, *Vol. 37, No. 4, pp. 318–325*

Figure 4. In reflected light, the lower cavity in the pavilion of this 3.30 ct diamond breaks the surface in a flower-like shape. Feathers can be seen extending from both cavities. A "spatter ring," a remnant of laser drilling, is also visible around the lower cavity. Magnified 160×.

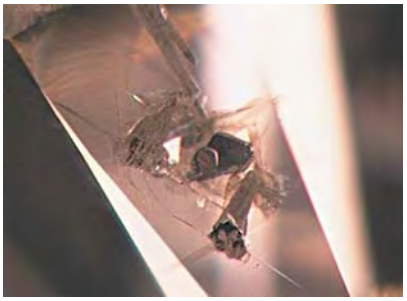

Figure 5. At 100× magnification with darkfield illumination, it is evident that the pavilion cavities in the diamond shown in figure 4 are cone shaped and reach a feather surrounding an included crystal.

Figure 6. The entry point on the crown best illustrates the fact that these cavities are the result of multiple laser drillings. Note the minute feathers extending off these tubes, which give them a "hairy" appearance. Magnified 100×.

4). Several feathers extended from both cavities on the pavilion, so that they appeared to be chips.

With darkfield illumination, magnification revealed that the two pavilion cavities extended into the stone in an inwardly tapering conical shape, and both touched a feather surrounding the same included crystal (figure 5). The roughness of the surfaces made the cavities look like indented naturals. However, our suspicions were aroused when we discovered that the cavity on the crown extended into the diamond via three separate conical tubes, two of which touched an internal feather surrounding a green crystal (figure 6). Along the length of each tube, and extending out from it, were minute feathers that gave the tubes a "hairy" appearance.

Our next task was to confirm that these conical tubes were laser drill holes and not natural etch channels. Etch channels in diamonds probably result from dissolution by corrosive fluids along weaknesses in the crystal structure (see, e.g., L. Orlov, *Mineralogy of the Diamond*, John Wiley & Sons, New York, 1977, pp. 98–100). Most commonly, their shape at the surface of the diamond, as well as the shape of the tube, is rhombic, square, rectangular, or hexagonal, due to the cubic crystal structure of diamond. In rare instances, such channels are triangular. The internal surfaces of etch channels may be smooth, or they may show transverse growth steps or parallel grooves (see, e.g., M. Johnson et al., "When a drill hole isn't," *Rapaport Diamond Report*, December 4, 1998, pp. 1, 19, 21, 23, 25–26).

Several features suggested that these tubes were not natural. They were oriented haphazardly to one another, and did not have any obvious relationship to the crystallographic orientation of the stone. Their shape was irregular at the surface of the diamond, and they narrowed into cones as they extended into the diamond, without any obvious growth steps. Also, their internal surfaces were rough, with a frosted appearance, and they contained small black spots. The last and most convincing piece of evidence was apparent only with high magnification: All three of the cavities were surrounded by "spatter rings" where they reached the surface of the diamond. These were created by carbon that was vaporized during the drilling process and redeposited around the outside of the drill hole (see, e.g., J. Koivula, "Micro evidence of natural diamond enhancement," *MicroWorld of Diamonds*, GemWorld International, Northbrook, IL, 2000, p. 110). This effect is best seen in figure 7 around the cavity in the crown. In our experience, these rings are not commonly seen due to the post-drilling repolishing of facets, but when present on a polished diamond they offer definitive evidence of laser drilling.

The unusual surface expressions of the cavities resulted from groups of drilled holes being aimed at a single point from slightly different angles.

Figure 7. When the laser-drilled diamond was examined with a combination of darkfield and reflected light, all three tubes could be seen associated with the crown cavity, as well as a "spatter ring" on the surface. Magnified 100×.

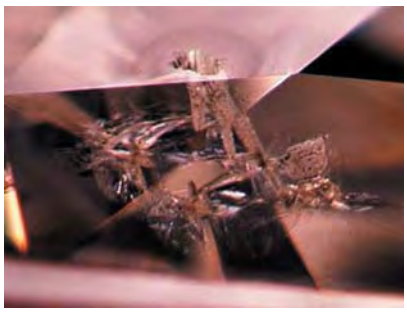

The flower-shaped cavity best illustrates this. The question remains: Why would someone do this to a diamond? Creating inclusions of this size hurt the clarity grade more than the crystals they were trying to reach. Perhaps the manufacturer was intentionally trying to make the laser drill holes look like indented naturals in a deceptive effort. Unfortunately, we will never know.

Wendi Mayerson

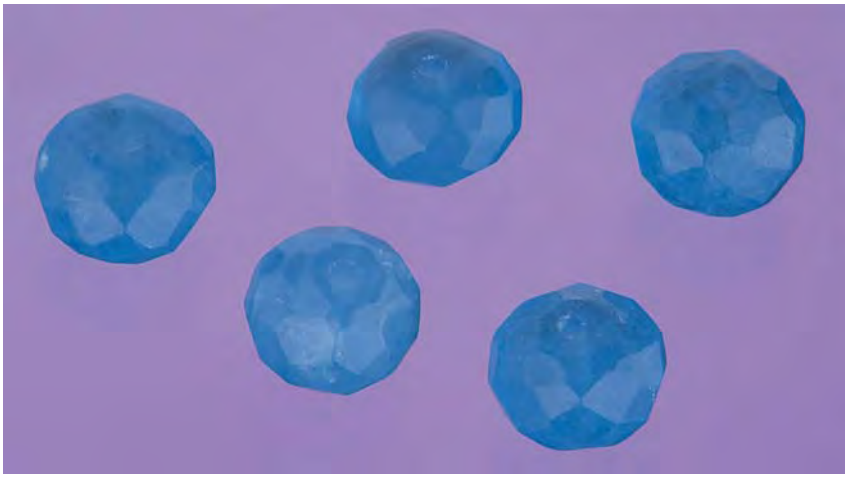

Figure 8. These five 8.0 × 4.8 mm faceted beads proved to be manufactured glass. They were represented as natural quartz from a "new locality" in China.

GLASS Sold as Quartz

A group of five faceted 8.0 × 4.8 mm translucent light blue button-shaped beads (figure 8) were sent to the West Coast lab by Patricia Gray of Graystone Enterprises in Missoula, Montana. She was suspicious of their nature, and curious about the inclusions they contained. The five beads, removed from a single-strand necklace, were purchased at the September 2001 Denver gem and mineral show, and were sold to Graystone as "natural blue quartz from a new undisclosed locality in China." Routine gemological testing proved that all five beads were manufactured glass.

When the beads were examined with magnification, numerous transparent rod-shaped to needle-like crystals were clearly and immediately visible (figure 9). In cross-section, these inclusions appeared to be diamond-shaped. When the crystals extended throughout the entire bead, they transmitted light—just as individual fiber-optic fibers would do—and they appeared colorless when examined down their length. This provided evidence that the beads derived their blue color from the glass body, not the inclusions. When examined with cross-polarized light, these inclusions responded in a manner consistent with doubly refractive crystals (figure 10).

Those inclusions exposed to the surface during polishing were raised above the surrounding glass, which indicates that they had a hardness greater than their host. The gas bubbles commonly associated with glass were scarce, although we observed occasional tiny individual bubbles between the rod-shaped inclusions or along grooves in their length (again, see figure 9). Laser Raman microspectrometry of the inclusions exposed to the surface gave a pattern for wollastonite (which has a reported hardness of 5–5 1/42 on the Mohs scale).

Wollastonite is a naturally occurring mineral, but in this instance the inclusions were undoubtedly a product of induced devitrification of the glass. This is not the first time synthetic wollastonite has been identified as inclusions in glass. For example, tabular crystals of synthetic wollastonite in glass are pictured in the *Photoatlas of Inclusions in Gemstones* (E. Gübelin and J.I. Koivula, ABC Edition, Zurich, 1986, p. 439); and, more recently, H. A. Hänni et al. reported on synthetic wollastonite inclusions in a glass that appears to be similar to the beads we examined ("A

Figure 9. All of the glass beads contained numerous inclusions identified as synthetic wollastonite. Note the tiny gas bubble trapped along a groove in one of the crystals (centered in the photo). Magnified 40×.

Figure 10. Cross-polarized light shows that the synthetic wollastonite inclusions are anisotropic. A first-order red compensator was used to shorten the exposure time. Magnified 35×.

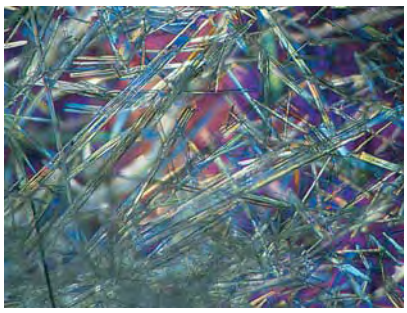

Figure 11. The animal figures (longest, 42.95 mm) in this necklace were represented as being carved from fossil ivory.

glass imitation of blue chalcedony," *Journal of Gemmology*, Vol. 27, No. 5, 2001, pp. 275–285). Whereas Dr. Hänni and his colleagues obtained their samples in Taiwan, represented as chalcedony, it appears that this material is now being sold—and misrepresented as quartz—in the U.S.

JIK and Maha Tannous

Fossil IVORY

Very little ivory has been submitted to the GIA Gem Trade Laboratory since importation of the material into the U.S. was banned in 1989. Therefore, it was interesting to receive for identification a necklace fashioned of numerous small carvings of animals (figure 11) that clearly exhibited the "engine-turned" structure (i.e., intersecting curved lines) characteristic of elephant ivory. The client's primary concern, however, was whether the necklace was recent or fossil ivory.

Fossil ivory typically comes from the woolly mammoth, an early relative of the modern elephant. Many of these mammoths, which became extinct about 10,000 years ago, died in the far northern latitudes, including Siberia, Alaska, and northern Canada. Because their ivory has been preserved in the continually frozen ground, this ancient material is often almost unchanged from the time it was buried; thus it can be cut, polished, and used in jewelry. Trade in fossil ivory is not regulated, as it poses no threat to the welfare of living elephants.

The challenge of separating modern ivory from mammoth ivory is that both materials exhibit the characteristic engine-turned structure (figure 12), and their gemological properties are virtually identical. However, John Koivula, GIA's chief research gemologist, recalled that several years ago he and former director of Gem Identification C. W. Fryer identified (using X-ray powder diffraction) a blue encrustation on some mammoth ivory as vivianite. This iron phosphate mineral formed via a chemical reaction with the phosphate in the ivory over an extended period of time. It is not present in recent ivory, so blue vivianite discolorations should prove that ivory is of ancient origin.

Fortunately, we were able to purchase a section of mammoth tusk, reportedly found in Canada's Yukon Territory, shortly after the necklace arrived in the lab. Readily visible on the weathered surface of this tusk section were several dark gray-blue smudges (figure 13). Closer inspection revealed a similarly colored encrustation on a broken surface and within several tiny cracks. Small pieces of the encrustation were scraped off and analyzed by laser Raman microspectrometry. The spectra were a perfect match for vivianite, confirming the results obtained years before by Koivula and Fryer. Consequently, we inspected our client's necklace for these blue smudges. We observed them, to some degree, in almost all the carved animals that made up the necklace, proving that this ivory was not of recent origin, but rather was fossil ivory. With magnification, the appearance of the vivianite ranged from small dots

Figure 12. This sample slab of mammoth ivory clearly shows the engine-turned effect in the darker internal layer of the tusk. The outer layer is cementum. Magnified 10×.

Figure 13. Note the irregular blue areas on the weathered surface of this section of mammoth tusk.

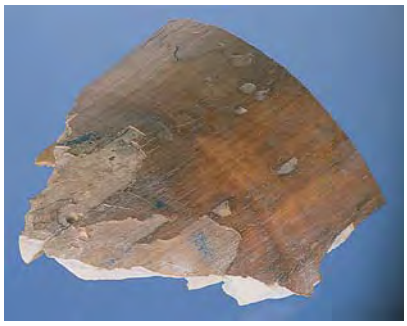

spread out or in dense groups to larger solid areas of a medium-blue to dark blue-gray color (figure 14).

We also noticed on the sample tusk section that there was a very thick (approximately 7 mm) layer on the outside of the tusk with a structure very different from its interior (again, see figure 12). This outside section, which is called "cementum," did not show the engine-turned effect, but instead had a layered structure that ran parallel to the length of the tusk. We found a layer of cementum in a section of modern elephant tusk, but it was very thin and difficult to see. Although additional research is needed, it is possible that the presence of a thick layer of cementum could also indicate mammoth ivory.

A paper published on the Web site for the National Fish and Wildlife Service (www.lab.fws.gov) described yet another way to distinguish recent elephant ivory from mammoth ivory. This paper states that the angles between the lines in the engine-turned effect (which they refer to as "Schreger lines") are different in these two types of ivory. Unfortunately, the process of obtaining these measurements is somewhat involved and requires a flat cross-section of a tusk, so this test would have limited value for ivory that has been carved or used in jewelry. Another advanced technique that has proved effective in separating elephant from mammoth ivory (as well as other ivory-like materials) is FT Raman (H. G. M. Edwards et al., "Fourier transform-Raman spectroscopy of ivory: A non-destructive diagnostic technique," *Studies in Conservation*, Vol. 43, No. 1, 1998, pp. 9–16). However, this technology is not readily available to most gemologists or gemological laboratories.

SFM

Figure 14. Vivianite in fossil ivory may appear as large areas with a fibrous structure that follows the structure of the host. Magnified 20×.

Hornbill "IVORY"

Recently, the West Coast lab was asked to identify a single 16.5 mm round bead that was semi-translucent to opaque light brownish yellow with a few "carmine" red to dark brown areas that gave it a marbled appearance (figure 15). Also eye-visible was a distinct difference in texture between: (1) an opaque, dense, featureless mass; and (2) a semi-translucent fibrous layered area. Closer observation with a standard gemological microscope revealed that the opaque mass contained very small particles that resembled granules of red pigment (figure 16). These particles were closely packed in the highly colored areas. Such characteristics can usually be found in various types of ivory and the rarely encountered hornbill "ivory."

Because the bead did not have a smooth finish, we had to check various areas before we were able to obtain a vague refractive index reading in the mid-1.50s, which is consistent with the reported values for hornbill "ivory." However, the fibrous area showed a slightly higher R.I., in the low 1.60s. When the bead was exposed to short-wave UV radiation, the light brownish yellow portion fluoresced chalky bluish white and the red area fluoresced strong red. The reaction to long-wave UV was even more intense. In addition, we noticed an odor similar to that of burnt hair when we touched the bead with a thermal reaction tester. Combined, these findings confirmed that the bead was fashioned from an organic material.

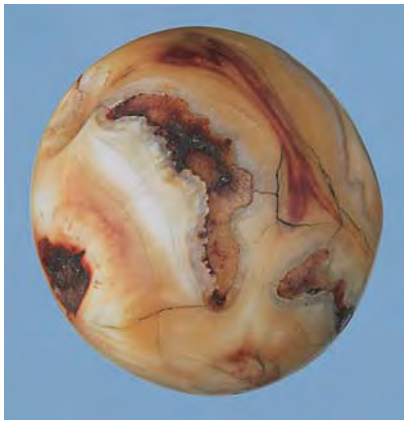

Figure 15. This 16.5 mm round bead was identified as hornbill "ivory."

The presence of the dark red area further proved that the bead had been carved from hornbill "ivory." This material is obtained from the casque of the helmeted hornbill, an exotic bird native to Borneo and Southeast Asia (see, e.g., R. E. Kane, "Hornbill ivory," Summer 1981 *Gems & Gemology*, pp. 96–97; G. Brown and A. J. Moule, "Hornbill ivory," *Journal of Gemmology*, Vol. 18, No. 1, 1982, pp. 8–19; and Lab Notes, Spring 1997, pp. 57–58, including the "editor's note" on trade restrictions). *KNH*

Figure 16. The "marbled" bead contained particles of red pigment that helped establish its organic nature and proved that it was hornbill "ivory." Magnified 15×.

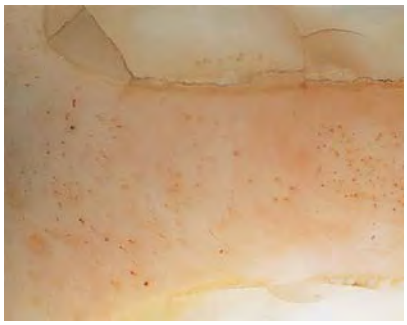

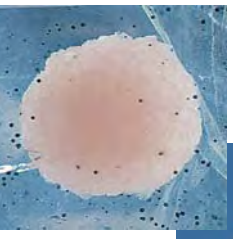

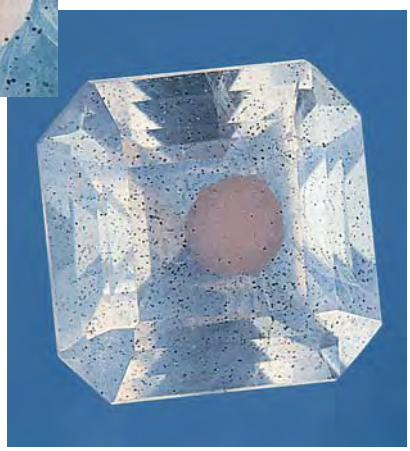

Figure 17. Almost centered in its 4.13 ct quartz host, the 3 mm mass of pink rhodochrosite makes this colorless gem very interesting. The faceted quartz also contains numerous tiny black crystallites of pyrrhotite, as shown in the inset.

QUARTZ with Rhodochrosite

As a faceted gemstone, rock crystal quartz is not particularly exciting unless it contains interesting inclusions. Such was the case with a 4.13 ct square emerald cut that was sent to the West Coast lab by gem dealer Elaine Rohrbach of Pittstown, New Jersey.

This 10.04 × 9.49 × 7.26 mm near-colorless gemstone contained an obvious pink, nearly spherical 3 mm mass under its table facet (figure 17). Even with the unaided eye, numerous tiny black crystallites were also clearly visible. The large pink mass was very close to the surface of the table, and a few of the black grains had been exposed to the surface during faceting. The near- or at-surface locations of these inclusions made them ideal for testing with the laser Raman microspectrometer. The Raman spectra revealed that the pink material was composed of the manganese carbonate rhodochrosite. The two tiny black grains that were analyzed individually proved to be the iron sulfide pyrrhotite.

Because the rhodochrosite inclusion was relatively large and close to the surface, we used EDXRF analysis to confirm its manganese content. With the aid of a masking technique to isolate the inclusion from the host quartz, this testing showed that the inclusion did indeed contain manganese as a major element. While the source of this unusual quartz is not known, we believe that it may have come from Mexico, specifically from the Gibraltar mine in Naica. As shown in figure 18, beautiful colorless crystals with rhodochrosite inclusions have been recovered from this locality.

JIK, Maha Tannous, and Sam Muhlmeister

Figure 18. It is possible that the gem in figure 17 was cut from rough similar to this 35.23-mm-long quartz cluster from the Gibraltar mine in Naica, Chihuahua, Mexico.

SAPPHIRES with Diffusion-Induced Stars

The East Coast lab recently received for identification two asteriated dark blue oval cabochons that weighed 31.64 ct and 15.26 ct, and measured 19.70 × 16.31 × 8.64 mm and 14.88 × 12.49 × 6.68 mm, respectively. In overhead reflected light, both cabochons appeared to be evenly colored and nearly opaque. The stars appeared white, with straight arms of equal length that seemed to float over the surface of the stones (figure 19). Typically, a six-rayed star forms as the result of reflections off three sets of oriented needles that are present

Figure 19. These semi-translucent to opaque dark blue star sapphires (31.64 and 15.26 ct) came into the East Coast lab for identification.

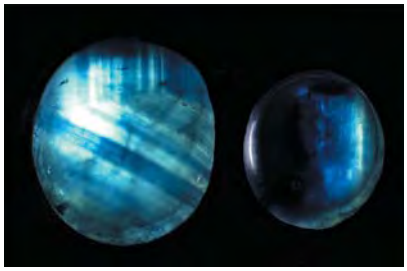

Figure 20. The straight, angular color zoning visible in transmitted light indicates that the dark blue color of these cabochons is natural.

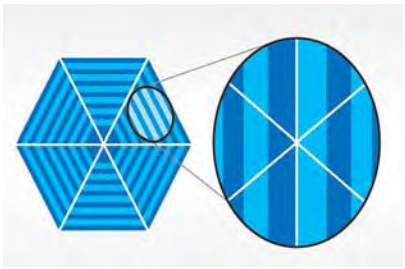

Figure 21. This line drawing illustrates the relationship between asterism and color zoning in a natural star sapphire (shown in both a rough crystal section and a polished cabochon). Note that two of the six rays are always parallel to the color zoning.

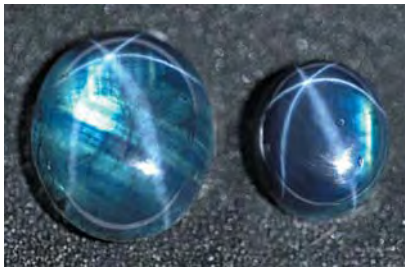

Figure 22. With combined transmitted and overhead lighting, it was evident that none of the rays of the stars was parallel to the hexagonal color banding. This was a strong indication that the stars were not natural.

throughout a large portion of the stone. Although examination in transmitted light revealed opaque and translucent areas along with straight, angular color banding (figure 20), we did not see any oriented needle-like inclusions with magnification. Aware that diffusion-induced asterism has been around since Linde Air Products Company patented the process in 1954 (as described in K. Nassau, "Heat treating ruby and sapphire: Technical aspects," Fall 1981 *Gems & Gemology*, pp. 121–131), we suspected that the two stones had been treated.

Standard gemological testing produced the following information on both stones: spot refractive indices of 1.76, no fluorescence to either long- or short-wave UV radiation, and a solid, heavy band from 450 to 470 nm that was visible in the desk-model spectroscope and was probably due to trace amounts of iron. Standard magnification (10×–60×) revealed melted fingerprint-like inclusions, polysynthetic twinning nearly parallel to the bases of the cabochons, and (as noted above) straight, angular bands that were either a very saturated dark blue or colorless—but no oriented needle-like inclusions. This combination of properties and features indicated that the stones were natural sapphires but the stars were manufactured.

In a sapphire with a natural star, the orientation of the asterism-causing needles is directly related to the crystallography of the host stone. Because color zoning is also related to the hexagonal crystal structure, the rays of the stars are always parallel to the six sides of the hexagon created by the growth/color zoning (see figure 21). Even if only one section of zoning is visible, as seen in the smaller of the two cabochons, two of the star's six rays would still be parallel to the visible banding. As is evident in figure 22, however, that was not the case for the stars on these cabochons. Therefore, we were not surprised when fiber-optic lighting revealed a very shallow hazy, whitish surface layer on both stones. Such a layer, composed of tiny individual needles too small to be detected at standard gemological magnification, previously has been associated with diffusion-induced stars (see, e.g., Lab Notes—Summer 1982, pp.106–107; Summer 1985, pp. 112–113; Fall 1985, pp. 171–172; Spring 1991, pp. 44–45; and Spring 1995, pp. 56–57; and Gem News—Summer 1996, pp. 136–137; and Winter 1997, pp. 308–309). Combined, the above findings allowed us to conclude that the stars on these cabochons had been artificially applied by means of a surface diffusion process.

It is particularly interesting that the treatment in these two cabochons consisted only of the creation of the stars, since the Gem Trade Laboratory more commonly sees this process on cabochons in which the color also has been diffusion-induced.

Wendi Mayerson

PHOTO CREDITS
Maha Tannous—figures 1, 2, 3, 8, 11, 13, 15, 17, and 18; Wendi Mayerson—figures 4, 5, 6, 7, and 21; John I. Koivula—figures 9, 10, 16, and 17 (inset); Shane F. McClure—figures 12 and 14; Elizabeth Schrader—figures 19, 20, and 22.